Journal of Sound and Vibration (2002) **251**(2), 241–259
doi:10.1006/jsvi.2001.3988, available online at http://www.idealibrary.com on IDEAL®

THE CHARACTERISTIC RECEPTANCE METHOD FOR DAMAGE DETECTION IN LARGE MONO-COUPLED PERIODIC STRUCTURES

H. Zhu and M. Wu

School of Civil Engineering, Huazhong University of Science and Technology, Wuhan 430074, People's Republic of China. E-mail: hpzhu@mail.hust.edu.cn

(*Received* 27 *February* 2001, *and in final form* 16 *July* 2001)

An approach based on the concept of wave propagation to detect the structural damage in large mono-coupled periodic structures is presented in this paper. The free vibration analysis of a finite mono-coupled periodic structure with a single disorder has been conducted by the characteristic receptance method, and the sensitivity of the natural frequencies to the disorder in flexibility has been discussed. Based on the sensitivity analysis, the locations and magnitude of damage in large mono-coupled periodic systems have been estimated using measured changes in the natural frequencies. The paper also introduces a substructure-based method for improving the computational efficiency and the accuracy of damage detection in large mono-coupled periodic structures. Numerical results from two periodic mass-spring-structures show that the proposed method can provide good predictions of both the locations and magnitude of damage at one or more sites. Furthermore, the proposed method, in which *a priori* information about the nature such as stiffness of the undamaged structure is not needed, and only measurements of the change in a few of the structure's natural frequencies between the undamaged and damaged states are required, is particularly attractive in practice. However, some issues such as the role of noise in actual measurements, application to multi-coupled periodic structures with complex boundary conditions remain to be resolved before this approach becomes a truly variable method of structural damage assessment.

1. INTRODUCTION

A periodic structure consists fundamentally of a number of identical structural components ("periodic element") which are joined together end-to-end and/or side-by-side to form the whole structure. Engineering structures including multi-storey buildings, elevated guideways for high-speed transportation vehicles ("Maglev" systems), multi-span bridges, multi-blade turbines and rotary compressors, chemical pipelines, stiffened plates and shells in aerospace and ship structures, the proposed space station structures and layered composite structures, can be considered as periodic systems. Accurate wave analysis for the free vibration of periodic structures not requiring the complete modelling of the structure is very appealing. The free vibration analysis of a periodic structure has been extensively investigated by many authors using different techniques such as the receptance method, the direct solutions for the response and propagation constants, the transfer matrix method, and the method of space-harmonics [1].

However, due to manufacturing errors and damages, in real structures, no periodic elements can be perfectly identical. For some periodic structures, the presence of small

0022-460X/02/120241 + 19 $35.00/0

irregularities may significantly affect natural frequencies and modal shapes of the structures. The most important effects of disorder include the localization of the natural modes of vibration to small geometric regions. In solid-state physics, the localization phenomenon of an electron field in disordered solids was first observed by Anderson [2], who shared the 1977 Nobel Prize in physics for his work. The localization phenomenon in engineering structures has been recently the focus of a number of theoretical investigations, and several theoretical methods have been applied to study this topic. Mead and Bansal [3] examined the effect of a single length disorder on the propagating wave motion along an infinite simply supported periodic beam by means of receptance methods. Kissel [4] used a travelling wave approach to investigate the localization effects on one-dimensional periodic engineering structures. Furstenberg's theorem on products of random matrices was applied to calculate the localization factor as a function of frequency by Ishii [5], while Herbert and Jones [6] and Thouless [7] employed a Green function formulation to study the same systems and obtained expressions for the localization factors. Cai and Lin [8] developed a new perturbation scheme to calculate the localization factor based on a generic periodic structure. Finally, Lust *et al.* [9] studied localization in a Timenshenko multi-span beam using the finite element method.

From the above statement, when a periodic structure suffers localized damage, its dynamic characteristics such as natural frequencies and modal shapes can change. Conversely, if the information about changes of modal parameters is available, the changes of stiffness caused by damage in the structure can be identified using an appropriate method. Several approaches of structural damage detection based on modal test data have been proposed and developed in the past 20 years, and the study on this topic is still active. These approaches can be generally classified into three categories: sensitivity-based method [10], optimization-technique-based method [11], non-parametric damage detection method such as neural networks [12]. The effectiveness of some of these techniques has been verified on simple structures such as beams, and low and middle frame structures. However, for a complex structure with a large number of degrees of freedom, such as a long-span bridge, a space truss and a highrise building, damage detection becomes difficult and time consumptive. Moreover, the incompleteness of the available modal test data becomes a considerable problem since the number of d.o.f. readings measured from modal testing is significantly smaller than the number of d.o.f.s in the analytical model of large structures. Although the problem can be solved by using either a model reduction technique or a mode shape expansion technique, it has often been pointed out that the model reduction process introduces errors in an analytical model and destroys the connectivity of the original model, whereas the mode shape expansion process introduces additional errors in the expanded mode shapes which directly affect the accuracy of the estimation of structural damage [11].

It is widely recognized that the natural frequencies are least contaminated by measurement noise and can generally be measured with good accuracy. In contrast, accurate measurements of mode shapes would be practically impossible [13]. In practice, measurements yield only partial modal shapes with respect to the total d.o.f. present in the corresponding analytical models. As a result, a method capable of predicting the magnitude as well as the location of damage that requires only the changes in the natural frequencies would be welcomed. Some researchers have proposed several approaches to locate the damage site by using the test natural frequencies [14, 15]. Experiments performed by Biswas *et al.* [16] on a highway bridge also demonstrated that changes in the natural frequencies alone could be used to detect damage.

The sensitivity-based method has been proved as an effective tool to find the changes of structural parameters which can directly affect the dynamic characteristics of a large

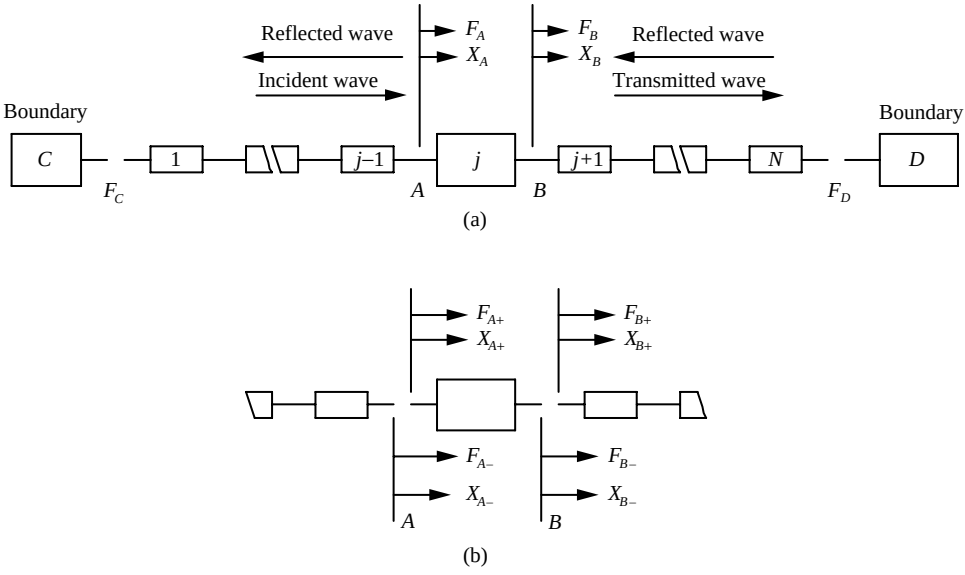

Figure 1. Block diagram of a finite mono-coupled periodic system of N elements and arbitrary boundaries with a disorder: (a) excitation F_C at end C and the responses at coupling co-ordinates of the disorder, (b) forces and displacements at connecting ends of the disorder.

structure. Cawley and Adams [17] used the first order perturbation of the basic eigenvalue equation to arrive at sensitivities necessary to locate the damage in a structure using natural frequencies. Stubbs [18] detected construction errors of large space structures by solving the sensitivity equations that were found analytically by computing the fractional change in the ith eigenvalue due to unit stiffness reduction at location j. The main disadvantage of these methods is that they are computationally expensive for large complex structures, because a detailed analytical model is required for an accurate localization.

In this paper, the characteristic receptance method is used to analyze the free wave motion of large mono-coupled periodic structures of N elements, and to yield the relationship between the changes of the receptances of periodic element and the natural frequencies of the periodic structure. The result is a set of simultaneous equations that relate the changes in the natural frequencies to those of the element flexibility. Then, given a set of measured decreases in the natural frequencies, the increase in the flexibility of each element can be obtained by solving this set of equations. In addition, a substructure-based method has been provided to improve the computational efficiency for the damage detection in large mono-coupled periodic structures. The accuracy of this proposed method is illustrated by detecting simulated damage at one or more sites in two different periodic mass–spring systems with one fixed end and one free end. From the numerical analysis, it can be noted that the combination of substructure theory and the characteristic receptance method can involve significant computational effort while maintaining the accuracy of damage detection when analyzing large mono-coupled periodic structures.

2. FREE WAVE PROPAGATION IN DISORDERED MONO-COUPLED PERIODIC STRUCTURES OF N ELEMENTS

Consider a finite mono-coupled periodic system having a single disorder in the jth element and terminating at the general boundaries at extreme end co-ordinates C and D as shown in Figure 1. Suppose that the finite system has N elements, and is excited by the force

F_C at the left-hand end, C. In the first place, boundary C is assumed to be disconnected. The free incident wave travels towards and impinges upon the disorder. Here, it is partially reflected back towards the source of excitation and partially transmitted across the disorder. The transmitted wave propagates on the right of the disorder, and then is partially reflected at the other end D. Thus, the total wave motion generated can be expressed as the sum of those corresponding to the transmitted and the reflected waves. Let the contributions to the total displacement and force at C from these two waves be X_{Ct} and X_{Cr}, so that

$$X_C = X_0 = X_{Ct} + X_{Cr}, \qquad F_C = F_0 = F_{Ct} + F_{Cr}, \tag{1}$$

where F_{Ct} and F_{Cr} are the generalized forces corresponding to the transmitted and reflected waves at end C respectively.

The displacement of the transmitted (incident) and reflected waves at the left junction A of the disorder element is

$$X_{A-t} = X_{Ct}\mathrm{e}^{-(j-1)\mu}, \qquad X_{A-r} = X_{Cr}\mathrm{e}^{(j-1)\mu},$$

where μ is the propagation constant of free wave motion.

The total displacement and force at junction A are

$$X_{A-} = X_{A-t} + X_{A-r} = X_{Ct}\mathrm{e}^{-(j-1)\mu} + X_{Cr}\mathrm{e}^{(j-1)\mu}, \qquad F_A = F_{At} + F_{Ar}, \tag{2a,b}$$

where F_{At} and F_{Ar} are the generalized forces corresponding to the transmitted and reflected waves at junction A.

Similarly, the displacement and force at the right junction B of the disorder element are

$$X_{B+} = X_{B+t} + X_{B+r} = X_{Dt}\mathrm{e}^{(N-j)\mu} + X_{Dr}\mathrm{e}^{-(N-j)\mu}, \qquad F_B = F_{Bt} + F_{Br}, \tag{3a,b}$$

where X_{Dt} and X_{Dr} are the displacements corresponding to the transmitted and reflected waves at end D.

With use being made of the concept of characteristic wave receptance [3] equations (2a) and (3a) can now be written as

$$X_{A-} = \alpha_{wt}F_{At} + \alpha_{wr}F_{Ar}, \qquad X_{B+} = \alpha_{wt}F_{\mathrm{Bt}} + \alpha_{wr}F_{Br} \tag{4a,b}$$

According to the definition of receptance, the displacements X_{A+} and X_{B-} at the two junctions A and B of the disorder element can be expressed as

$$X_{A+} = \alpha_{AA}F_{A+} + \alpha_{AB}F_{B-}, \qquad X_{B-} = \alpha_{BA}F_{A+} + \alpha_{BB}F_{B-}, \tag{5a,b}$$

where α_{AA}, α_{BB} are the direct receptances and α_{AB}, α_{BA} are the transfer receptances of the disorder element.

For compatibility of the displacements and equilibrium of the forces at junctions A and B, one has

$$X_{A+} = X_{A-}(= X_A = X_{j-1}, say), \qquad X_{B+} = X_{B-}(= X_B = X_j, say),$$
$$F_{A+} = -F_{A-}(= F_A = F_{j-1}, say), \qquad F_{B+} = -F_{B-}(= F_B = F_j, say).$$

Thus, equations (5) can be rewritten in the form

$$X_A = \alpha_{AA}F_A - \alpha_{AB}F_B, \qquad X_B = \alpha_{BA}F_{\mathrm{A}} - \alpha_{BB}F_B. \tag{6a,b}$$

Compared with equations (4) and (6), one finds, for compatibility at A and B,

$$(\alpha_{AA} - \alpha_{wt})F_{At} + (\alpha_{AA} - \alpha_{wr})F_{Ar} = \alpha_{AB}F_{Bt} + \alpha_{AB}F_{Br}, \tag{7a}$$

$$(\alpha_{BB} + \alpha_{wt})F_{Bt} + (\alpha_{BB} + \alpha_{wr})F_{Br} = \alpha_{BA}F_{At} + \alpha_{BA}F_{Ar}. \tag{7b}$$

By substituting $F_{At} = X_{At}/\alpha_{wt}, F_{Ar} = X_{Ar}/\alpha_{wr}, F_{Bt} = X_{Bt}/\alpha_{wt}, F_{Br} = X_{Br}/\alpha_{wr}$, and equations (2a) and (3a), equations (7) can be represented as

$$(\alpha_{AA} - \alpha_{w+})\frac{X_{0t}e^{-(j-1)\mu}}{\alpha_{wt}} + (\alpha_{AA} - \alpha_{wr})\frac{X_{0r}e^{(j-1)\mu}}{\alpha_{wr}} = \alpha_{AB}\frac{X_{Nt}e^{(N-j)\mu}}{\alpha_{wt}} + \alpha_{AB}\frac{X_{Nr}e^{-(N-j)\mu}}{\alpha_{wr}},$$

$$(\alpha_{BB} + \alpha_{w+})\frac{X_{Nt}e^{(N-j)\mu}}{\alpha_{wt}} + (\alpha_{BB} + \alpha_{wr})\frac{X_{Nr}e^{-(N-j)\mu}}{\alpha_{wr}} = \alpha_{BA}\frac{X_{0t}e^{-(j-1)\mu}}{\alpha_{wt}} + \alpha_{BA}\frac{X_{0r}e^{(j-1)\mu}}{\alpha_{wr}}. \quad (8a,b)$$

The total displacement and force at the other end of the system, D, are

$$X_D = X_N = X_{Nt} + X_{Nr}, \qquad F_D = F_N = F_{Nt} + F_{Nr} = \frac{X_{Nt}}{\alpha_{wt}} + \frac{X_{Nr}}{\alpha_{wr}}. \quad (9a,b)$$

Suppose that the receptance at end D is α_D, the displacement X_D can be expressed in terms of the force F_D and α_D,

$$X_D = X_{Nt} + X_{Nr} = \alpha_D F_D \quad (9c)$$

Eliminating F_D from equations (9b,c), one finds the ratio, β, of the displacements at junction D associated with the transmitted and reflected waves to be

$$\frac{X_{Nt}}{X_{Nr}} = -\frac{\alpha_{wr} - \alpha_D}{\alpha_{wt} - \alpha_D}\frac{\alpha_{wt}}{\alpha_{wr}} = \beta. \quad (10)$$

Substitution of equation (10) into equations (8) yields

$$X_{Nr} = \frac{\alpha_{wr}(\alpha_{AA} - \alpha_{wt})e^{-(j-1)\mu}X_{0t} + \alpha_{wt}(\alpha_{AA} - \alpha_{wr})e^{(j-1)\mu}X_{0r}}{\alpha_{AB}[\alpha_{wr}e^{(N-j)\mu}\beta + \alpha_{wt}e^{-(N-j)\mu}]}, \quad (11a)$$

$$X_{Nr} = \frac{\alpha_{BA}\alpha_{wr}e^{-(j-1)\mu}X_{0t} + \alpha_{BA}\alpha_{wt}e^{(j-1)\mu}X_{0r}}{(\alpha_{BB} + \alpha_{wt})\alpha_{wr}\beta e^{(N-j)\mu} + (\alpha_{BB} + \alpha_{wr})\alpha_{wt}e^{-(N-j)\mu}}. \quad (11b)$$

The ratio, Φ, of X_{0r} to X_{0t} can be obtained by equalizing equations (11a) and (11b),

$$\frac{X_{0r}}{X_{ot}} = \Phi = -\frac{\begin{array}{c}[\alpha_{AA}\alpha_{BB} - \alpha_{BA}\alpha_{AB} + \alpha_{AA}\alpha_{wt} - \alpha_{BB}\alpha_{wt} - \alpha_{wt}^2]\alpha_{wr}^2\beta e^{(N-2j+1)\mu} \\ + [\alpha_{AA}\alpha_{BB} - \alpha_{AB}\alpha_{BA} + \alpha_{AA}\alpha_{wr} - \alpha_{BB}\alpha_{wt} - \alpha_{wt}\alpha_{wr}]\alpha_{wr}\alpha_{wt}\beta e^{-(N-t)\mu}\end{array}}{\begin{array}{c}[\alpha_{AA}\alpha_{BB} - \alpha_{BA}\alpha_{AB} + \alpha_{AA}\alpha_{wr} - \alpha_{BB}\alpha_{wr} - \alpha_{wr}^2]\alpha_{wt}^2 e^{-(N-2j+1)\mu} \\ + [\alpha_{AA}\alpha_{BB} - \alpha_{AB}\alpha_{BA} + \alpha_{AA}\alpha_{wt} - \alpha_{BB}\alpha_{wr} - \alpha_{wt}\alpha_{wr}]\alpha_{wr}\alpha_{wt}\beta e^{(N-1)\mu}\end{array}} \quad (12)$$

The characteristic receptances of the two waves are given by [3]

$$\alpha_{wt} = \alpha_{ll} - \alpha_{lr}e^{-\mu}, \qquad \alpha_{wr} = \alpha_{ll} - \alpha_{lr}e^{\mu}, \quad (13)$$

where α_{ll} and α_{lr} are the direct and transfer receptances of the periodic element respectively.

Equation (12) can be verified by assuming that there is no disorder in the system with symmetric periodic elements. With the symmetric element the receptances of the periodic system satisfy

$$\alpha_{AA} = \alpha_{BB} = \alpha_{ll} \quad \text{and} \quad \alpha_{AB} = \alpha_{BA} = \alpha_{lr}. \quad (14)$$

Moreover, assuming that the system is free at end D, such that $\alpha_D = \infty$, equation (12) can be simplified by substituting equations (13) and (14) into equation (12)

$$X_{0r} = -\left(\frac{\alpha_{wr}}{\alpha_{wt}}\right)X_{0t}e^{-2N\mu} \quad (15)$$

which coincides with equation (21) in reference [3].

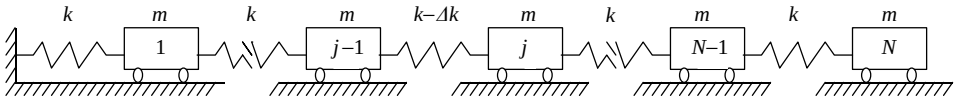

Figure 2. The N-element periodic mass–spring system with a single disorder of stiffness in the jth element which is fixed at left end and free at the right end.

From equation (12), the total displacement at end C is

$$X_C = X_0 = X_{0t} + X_{0r} = (1 + \Phi)X_{0t} \tag{16}$$

By combining equations (10), (11a), (12) and (16), one finds the displacement at D

$$X_D = X_N = \frac{(1+\beta)[\alpha_{wr}(\alpha_{AA} - \alpha_{wt})e^{-(j-1)\mu} + \alpha_{wt}(\alpha_{AA} - \alpha_{wr})\,e^{(j-1)\mu}\Phi]}{(1+\Phi)\,\alpha_{AB}\,[\alpha_{wr}\,e^{(N-j)\mu}\beta + \alpha_{wt}\,e^{-(N-j)\mu}]}\,X_0\,. \tag{17}$$

The displacement X_i at arbitrary junction i is

$$X_i = X_{it} + X_{ir} = X_{0t}e^{-i\mu} + X_{0r}e^{i\mu} = \frac{e^{-i\mu} + \Phi e^{i\mu}}{1+\Phi}X_0 \quad (i = 1, 2, \ldots, j-1), \tag{18a}$$

$$X_i = X_{it} + X_{ir} = X_{Nt}e^{(N-i)\mu} + X_{Nr}e^{-(N-i)\mu} = \frac{\beta e^{(N-i)\mu} + e^{-(N-i)\mu}}{1+\beta}\,X_N$$

$$= \frac{(e^{-(N-i)\mu} + \beta e^{(N-i)\mu})[\alpha_{wr}(\alpha_{AA} - \alpha_{wt})e^{-(j-1)\mu} + \alpha_{wt}(\alpha_{AA} - \alpha_{wr})\,e^{(j-1)\mu}\Phi]}{(1+\Phi)\,\alpha_{AB}\,[\alpha_{wr}\,e^{(N-j)\mu}\beta + \alpha_{wt}\,e^{-(N-j)\mu}]}\,X_0$$

$$(i = j, j+1, \ldots, N)\,. \tag{18b}$$

For a finite value of X_0, the displacements at arbitrary junctions can be infinite when the denominator of equations (18) is zero. This occurs at a frequency which satisfies

$$1 + \Phi = 0\,. \tag{19}$$

3. APPLICATION TO PERIODIC MASS–SPRING SYSTEMS WITH A SINGLE DISORDER

The above analysis is quite general and can be applied to study various types of finite mono-coupled periodic systems with a single disorder. However, the theory developed above will be applied here only to study periodic mass–spring systems with one disorder (i.e., disorder of flexibility). Typically, the shearing model of multi-storey buildings can be represented by the mass–spring system; in this case, the generalized forces and displacements will be the shearing forces and horizontal displacements of each storey.

Figure 2 shows the N-element periodic mass–spring system with one fixed end C and one free end, D (i.e., $\alpha_D = \infty$). This finite periodic structure has one disorder in the jth element, and only disorder of flexibility is considered.

The receptances of the periodic element can be expressed as

$$\alpha_{ll} = \frac{m\omega^2 - k}{m\omega^2 k} = f - \frac{1}{m\omega^2}, \qquad \alpha_{rr} = \alpha_{lr} = \alpha_{rl} = -\frac{1}{m\omega^2}, \tag{20}$$

where m, k, and f are the mass, stiffness and flexibility of one mass–spring element, respectively, and ω is vibration circular frequency.

The receptances of the disorder element (i.e., the jth element) are

$$\alpha_{AA} = f + \Delta f - \frac{1}{m\omega^2} = \alpha_{ll} + \Delta f, \qquad \alpha_{AB} = \alpha_{BA} = \alpha_{BB} = -\frac{1}{m\omega^2}, \tag{21}$$

where Δf is the change of flexibility in the jth element.

By substituting equations (12), (13), (20) and (21) into equation (19), and after some manipulation, the characteristic equation of natural frequencies of the periodic mass–spring structure with a single disorder can be obtained:

$$\cos\tfrac{\gamma}{2}\cos[(N + 0{\cdot}5)\gamma] - \frac{2\Delta f}{f}\sin\tfrac{\gamma}{2}\sin[(N - j + 1)\gamma]\cos[(j - 0{\cdot}5)\gamma] = 0, \tag{22}$$

where $\gamma = \mathrm{i}\mu$ is also the wave propagation constant.

The characteristic equation of natural frequencies of the periodic mass spring structure without any disorders can be obtained by putting $\Delta f = 0$ in equation (22):

$$\cos\tfrac{\gamma}{2}\cos[(N + 0{\cdot}5)\gamma] = 0. \tag{23}$$

The propagation constant μ can be expressed in terms of the receptances of periodic element [3] as

$$\cosh\mu = \frac{(\alpha_{ll} + \alpha_{rr})}{2\alpha_{lr}}. \tag{24}$$

Substitution of equations (20) and $\gamma = \mathrm{i}\mu$ into equation (24) gives

$$\gamma = 2\arcsin\left(\frac{\omega}{2\omega_0}\right), \tag{25}$$

where $\omega_0 = \sqrt{k/m}$.

Application of equation (25) to equation (23) yields the nth natural circular frequencies, $\omega_u^{(n)}$, of the N-element periodic structure without any disorders

$$\omega_u^{(n)} = 2\sqrt{\frac{k}{m}}\sin\left[\frac{\pi}{2}\frac{2n-1}{2N+1}\right] \quad (n = 1, 2, \ldots, N) \tag{26}$$

which is the same as equation (9) in reference [19].

Substitution of equation (26) into equation (25) leads to the wave propagation constant at the nth natural frequency

$$\gamma_u^{(n)} = \frac{(2n-1)\,\pi}{2N+1}. \tag{27}$$

Let $\delta\gamma_j^{(n)}$ be the change of $\gamma_u^{(n)}$ due to a small flexibility change, $\delta\xi_j = \delta f/f$, in the jth element. Substitution of $\gamma = \gamma_u^{(n)} + \delta\gamma_j^{(n)}$ into equation (23) gives, after some manipulation,

$$\begin{aligned}
&\cos\left[\frac{\pi}{2}\frac{2n-1}{2N+1}\right]\sin[(N+0.5)\delta\gamma_j^{(n)}] + \delta\xi_j\sin\left[\frac{\pi}{2}\frac{2n-1}{2N+1}\right]\cos[(N+0.5)\delta\gamma_j^{(n)}] \\
&\quad + \delta\xi_j\sin\left[\frac{\pi}{2}\frac{2n-1}{2N+1}\right]\cos\left[(2j-1)\frac{2n-1}{2N+1}\right]\cos[(N+1{\cdot}5-2j)\delta\gamma_j^{(n)}] \\
&\quad + \delta\xi_j\sin\left[\frac{\pi}{2}\frac{2n-1}{2N+1}\right]\sin\left[(2j-1)\frac{2n-1}{2N+1}\right]\sin[(N+1{\cdot}5-2j)\delta\gamma_j^{(n)}] = 0.
\end{aligned} \tag{28}$$

Solving equation (28) yields $\delta\gamma_j^{(n)}$, due to disorder at the jth element, $\delta\xi_j$. From equation (28), it can be seen that the change, $\delta\gamma_j^{(n)}$, depends only on the disorder element number (j) and the number of the element of the periodic system (N). That is, prior information about the structure nature such as m and k does not influence the change.

The change, $\delta\omega_j^{(n)}$, of the nth natural circular frequency due to $\delta\gamma_j^{(n)}$ can be found by solving equation (25),

$$\delta\omega_j^{(n)} = 2\sqrt{\frac{k}{m}}\sin\left(\frac{\delta\gamma_j^{(n)}}{2}\right). \tag{29a}$$

Combining equations (26) and (29a) gives the relative change of the nth natural circular frequency due to the disorder in the jth element:

$$\delta\bar{\omega}_j^{(n)} = \frac{\delta\omega_j^{(n)}}{\omega^{(n)}} = \frac{\sin\left(\dfrac{\delta\gamma_j^{(n)}}{2}\right)}{\sin\left[(\pi/2)\dfrac{(2n-1)}{(2N+1)}\right]}. \tag{29b}$$

It is assumed that damage to the jth element is simulated by a homogeneous reduction of stiffness (i.e., increase of flexibility), but with no change of mass. In this case, the sensitivity of the nth natural circular frequency to damage at element j is given by the equation

$$\frac{\partial\bar{\omega}^{(n)}}{\partial\xi_j} = \lim_{\delta\xi_j\to 0}\frac{\delta\bar{\omega}_j^{(n)}}{\delta\xi_j} = \lim_{\delta\xi_j\to 0}\frac{\sin\left(\dfrac{\delta\gamma_j^{(n)}}{2}\right)}{\delta\xi_j\sin[(2n-1)\,\pi/2(2N+1)]} \quad (j = 1, 2, \ldots, N). \tag{30}$$

As indicated in equation (28), equation (30) tells us again that for a periodic mass–spring system, the sensitivity of natural frequency to damage depends only on the number of the element of the periodic system and the location of disorder, it does not depend on the structural parameters such as the stiffness and mass of the periodic system.

Figure 3(a, b) shows the sensitivity of the first five natural frequencies of the periodic mass spring systems of 10 and 20 elements to the locations of disorder respectively. From these figures, it can be noted that for each natural frequency, there are some locations where the frequency is most sensitive to the disorder, while there are also some locations in which the disorder makes little influence on the frequency. Furthermore, for a specified natural frequency, the number of elements with the highest sensitivity does not depend on the parameters of the system such as m, k, and N, but only on this natural frequency's number. For example, the influence of disorder on the first natural frequency decreases as the location of disorder approaches the free end, that is, the first natural frequency is most sensitive to damage in the element adjacent to the fixed end. For the second natural frequency, there are two peaks (at element 1 and adjacent elements 7, 8) where the frequency is most sensitive. Similarly, for the third, fourth and fifth frequencies, the numbers of peaks are three, four and five, respectively, which are equal to the corresponding natural frequency numbers. The elements at or near to the peaks can be considered as the possible damage locations in the preliminary detection of the damage location by using the difference in the natural frequency between the undamaged and damaged states. The details will be demonstrated by analytical examples in the next section.

The flexibility increase factor $\delta\xi_j$ for the jth element is used to evaluate the degree of damage such that $\delta\xi_j = 0$ for no damage and $\delta\xi_j = \infty$ for complete loss of the element

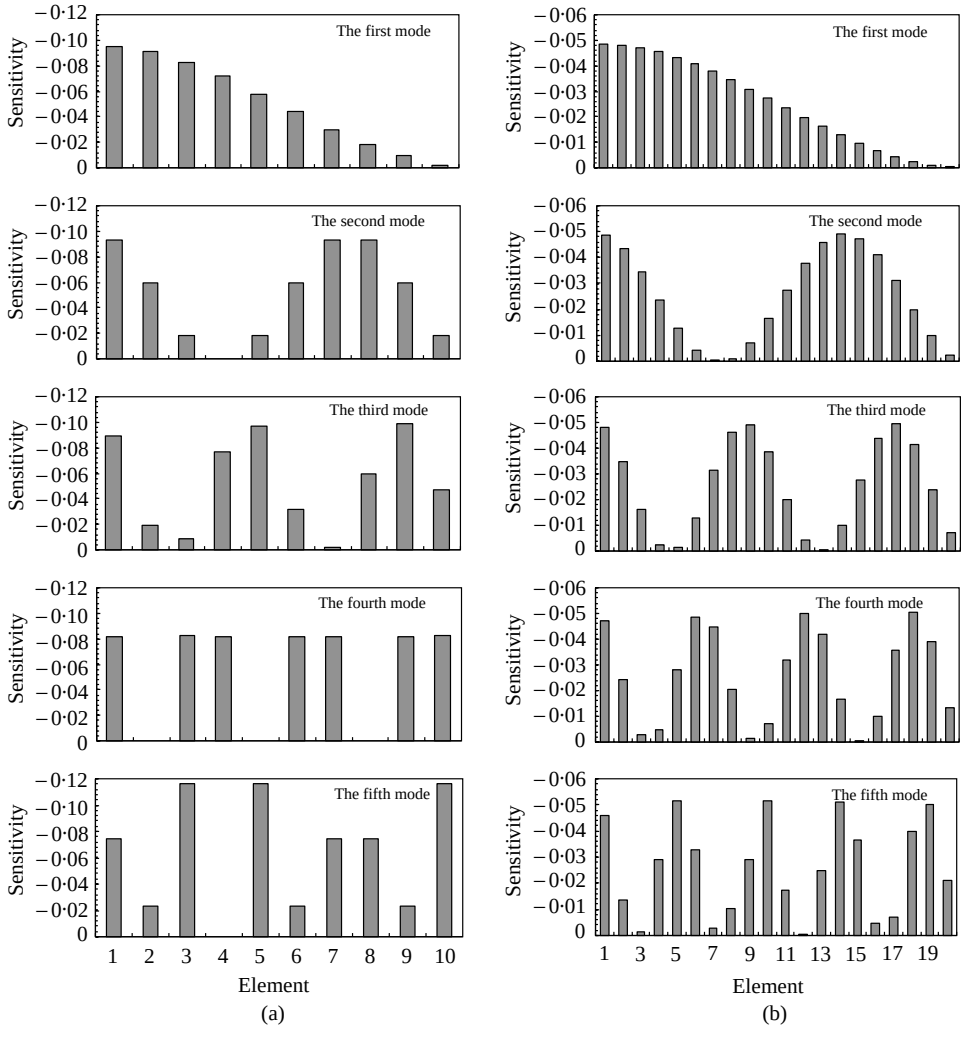

Figure 3. The sensitivity of the first five natural frequencies to the disorder elements for the periodic mass–spring structures which is fixed at element 1 and free at element N: (a) $N = 10$; (b) $N = 20$.

(100% damage). For any combination of size and location of damage at one or more sites, it is assumed that the corresponding reductions in the natural frequencies can be written using a linear combination of the sensitivities in the form

$$\delta\bar{\omega}^{(1)} = \frac{\partial\bar{\omega}^{(1)}}{\partial\xi_1}\delta\xi_1 + \frac{\partial\bar{\omega}^{(1)}}{\partial\xi_2}\delta\xi_2 + \cdots + \frac{\partial\bar{\omega}^{(1)}}{\partial\xi_N}\delta\xi_N$$

$$\vdots$$

$$\delta\bar{\omega}^{(p)} = \frac{\partial\bar{\omega}^{(p)}}{\partial\xi_1}\delta\xi_1 + \frac{\partial\bar{\omega}^{(p)}}{\partial\xi_2}\delta\xi_2 + \cdots + \frac{\partial\bar{\omega}^{(p)}}{\partial\xi_N}\delta\xi_N$$

or

$$\{\delta\bar{\omega}\} = \begin{bmatrix} \dfrac{\partial\bar{\omega}^{(1)}}{\partial\xi_1} & \cdots & \dfrac{\partial\bar{\omega}^{(1)}}{\partial\xi_N} \\ \cdots & \cdots & \cdots \\ \dfrac{\partial\bar{\omega}^{(p)}}{\partial\xi_1} & \cdots & \dfrac{\partial\bar{\omega}^{(p)}}{\partial\xi_N} \end{bmatrix} \{\delta\xi\} \tag{31}$$

or

$$\{\delta\bar{\omega}\} = [\mathrm{S}]\{\delta\xi\}.$$

The set of simultaneous equations in equation (31) relate the change of the flexibility of each element, $\{\delta\xi\}$, to the changes in the natural circular frequency of the structure, $\{\delta\bar{\omega}\}$. In this problem, it is assumed that there are p natural frequencies of the damaged structure available through measurements. The solution of equation (31) yields the corresponding changes in the element flexibility. Theoretically, if the number of available changes in frequency, p, is equal to N, a solution may be determined uniquely. However, only a small number of natural frequencies can usually be measured. Hence, the number of measured changes is less than the number of elements, ($p \prec N$), which renders the equations underdetermined. They can be solved uniquely only after the introduction of an optimality criterion.

In this study, the optimization problem can be stated as follows to find the best approximations which minimize the next matrix norm:

$$g = \|[S]\{\delta\xi\} - \{\delta\bar{\omega}\}\|. \tag{32a}$$

Since a negative change in the flexibility can never be produced by damage, the inequality constraint given in equation (32b) is introduced:

$$\{\delta\xi\} \geqslant 0. \tag{32b}$$

Thus, to find the optimal solution for the changes in the element flexibility is really a procedure to solve the constrained least-squares problem [20]:

$$\text{minimize } \|[S]\{\delta\xi\} - \{\delta\bar{\omega}\}\| \text{ subject to } \{\delta\xi\} \geqslant 0. \tag{33}$$

In principle, all elements in the structure could be considered as potential damage sites. For a large and complex periodic structure, the optimum solution procedure is computationally expensive. However, the next section discusses a method of reducing computational effort by excluding elements that are unlikely to be damaged.

4. ANALYTICAL EXAMPLES

Two periodic mass–spring systems with one fixed end C and one free end D shown in Figure 2 are used to illustrate the versatility of the proposed method. The numbers of elements of the two periodic systems are 10 and 20 respectively. The latter is also used to introduce the way of improving the computational efficiency. Without loss of generality, frequency changes for the first five modes are used in the assessment of damage.

First, it is assumed that an analytical model exists that correctly describes the system before damage. So, all the natural frequencies are obtained by solving equation (26); consequently, the sensitivity matrix, $[S]$, is formed through calculating all the sensitivity terms, $\partial\bar{\omega}^{(n)}/\partial\xi_j (n = 1, 2, \ldots, p;\ j = 1, 2, \ldots, N)$, by using equation (30). Then a known increase in flexibility which is referred to here as the "actual" damage is induced at one or more elements of the periodic systems. The difference in the natural frequencies between the

TABLE 1

Damage scenarios for the 10*-element periodic mass–spring structure*

Cases	Case 1	Case 2	Case 3	Case 4	Case 5	Case 6	Case 7	Case 8	Case 9	Case 10	Case 11	Case 12
Damage element	1	5	10	1, 5	1, 10	1, 5, 10	1	5	10	1, 5	1, 10	1, 5, 10
$\delta\xi$			5%						30%			

TABLE 2

The changes in the first five natural frequencies due to damage for the 10*-element periodic mass–spring structure*

Mode	Relative change ($\delta\bar{\omega}$) of the natural frequencies in percentage due to damage											
	Case 1	Case 2	Case 3	Case 4	Case 5	Case 6	Case 7	Case 8	Case 9	Case 10	Case 11	Case 12
1	− 0·47	− 0·29	− 0·01	− 0·76	− 0·48	− 0·77	− 2·75	− 1·71	− 0·06	− 4·31	− 2·81	− 4·36
2	− 0·45	− 0·09	− 0·09	− 0·54	− 0·54	− 0·63	− 2·57	− 0·54	− 0·56	− 3·23	− 3·07	− 3·70
3	− 0·41	− 0·45	− 0·22	− 0·85	− 0·63	− 1·07	− 2·23	− 2·61	− 1·43	− 4·60	− 3·56	− 5·87
4	− 0·35	0·0	− 0·36	− 0·35	− 0·71	− 0·71	− 1·82	0·0	− 2·31	− 1·87	− 4·03	− 4·03
5	− 0·28	− 0·45	− 0·46	− 0·73	− 0·73	− 1·17	− 1·40	− 2·61	− 2·71	− 4·06	− 4·06	− 6·40

undamaged and damaged models is calculated. Assuming that this difference is the only known data, the increase in flexibility is calculated by solving the optimization problem of equation (33). The results of this calculation will be referred to as the "predicted" damage in this study.

4.1. EXAMPLE 1: A PERIODIC MASS–SPRING STRUCTURE OF 10 ELEMENTS

For the 10-element periodic mass–spring system, the mass and stiffness of each element are 1.0×10^5 kg and 1.7655×10^8 N/m, respectively. The method was tested for its ability to detect light or severe damage for 12 damage states (see Table 1). The calculated changes in the natural circular frequencies of the structure that was damaged at different cases are shown in Table 2. Using the calculated changes in the natural frequencies shown in Table 2, the location and magnitude of damage were identified with the theory developed herein.

In the stage of preliminary detection mentioned in the above section, the damage locations in some cases listed in Table 1 can be roughly identified by using the degree of sensitivity of disorder in different elements shown in Figure 3(a). For example, from Table 2, the difference in the natural frequencies decreases as the natural frequency number increases in cases 1 and 7, which matches the variation of sensitivity of natural frequency to the disorder of the first element. On the other hand, in cases 3 and 9, the difference in the first frequency is near zero, and as the natural frequency number increases, the difference in the natural frequencies increases. Thus, in the two cases, the disorder most probably occurs in the 10th element which has little effect on the first frequency, and whose influence on the frequency becomes large as the frequency number increases. In cases 2, 4, 6, 8, 10 and 12,

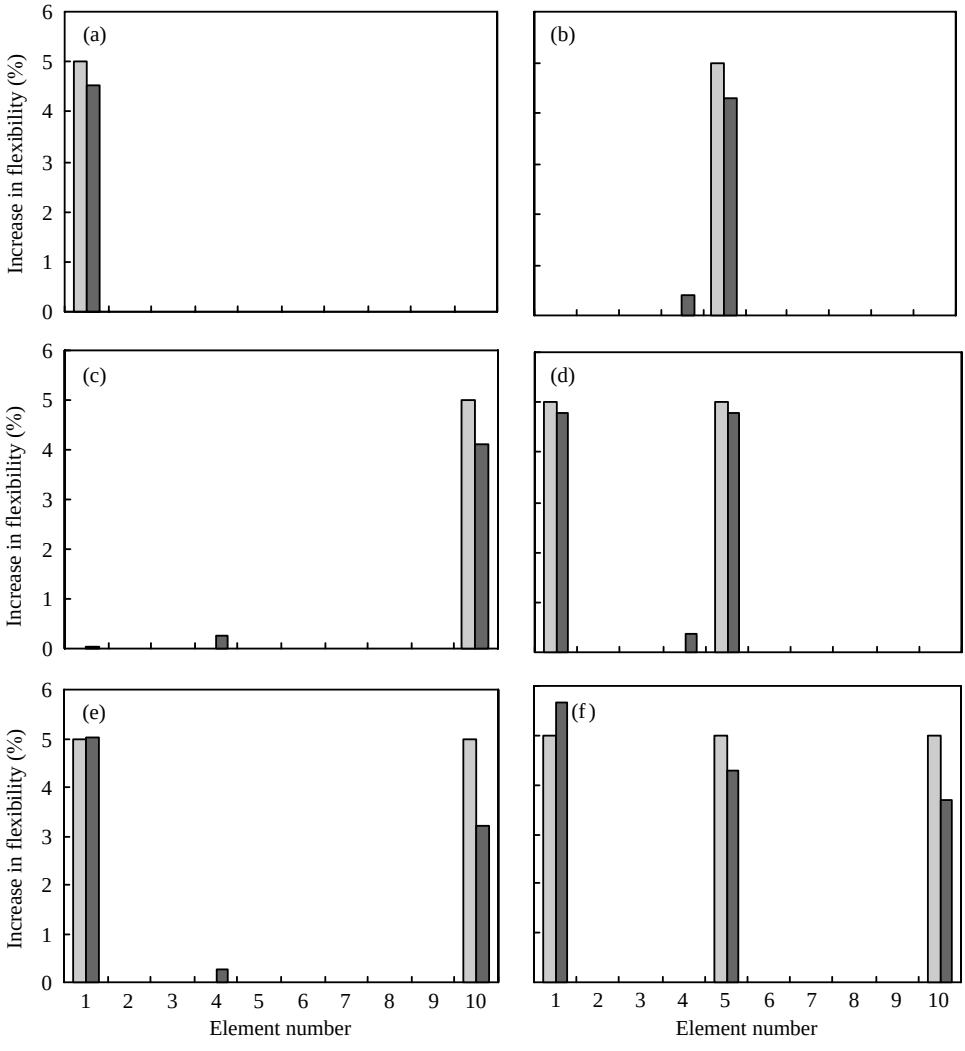

Figure 4. Detection of light damage of the 10-element periodic mass–spring structure at: (a) element 1, (b) element 5, (c) element 10, (d) elements 1 and 5, (e) elements 1 and 10, (f) elements 1, 5 and 10: ▒, actual damage; ■, Predicted damage.

the fact that the difference in the first, third and fifth frequencies is large indicates that the possible damage positions are elements 1 and 5. Moreover, in cases 2 and 8, the fact that the difference in the second frequency is small and the difference in the fourth frequency is near zero excludes element 1. Finally, from Figure 3(a), the damage in elements 1 and 10 most possibly produces the variation of the difference in the five frequencies in cases 5 and 11. Obviously, in the preliminary stage, relatively accurate detection of location for one damage can be achieved; however, for multiple damages, the magnitude of each damage makes the identification of damaged location complicated. The further detection of the location and magnitude of damages which requires solving the optimization problem of equation (33) is given below.

First, the flexibility of elements 1, 5 and 10 was increased by 5%. The results for damage of single element are shown in Figure 4(a–c) respectively. Detection of multiple damage of

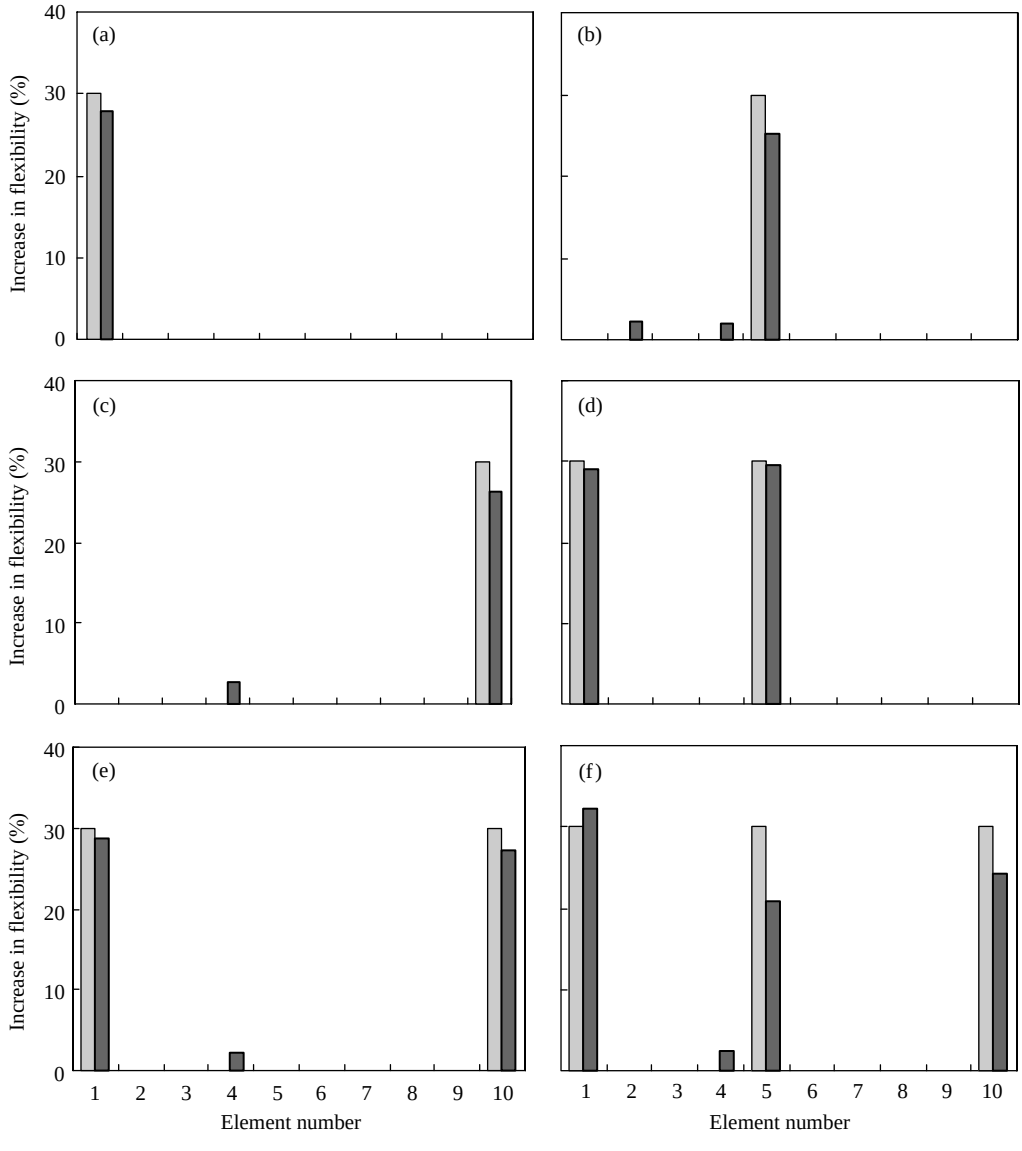

Figure 5. Detection of severe damage of the 10-element periodic mass–spring structure at: (a) element 1, (b) element 5, (c) element 10, (d) elements 1 and 5, (e) elements 1 and 10, (f) elements 1, 5 and 10 ▒, actual damage; ■, Predicted damage.

the structure is shown in Figure 4(d–f). It can be seen that both the location and the magnitude of the light damage were predicted reasonably well in all cases. The process was repeated for detection of severe damage. The flexibility of the damaged elements was increased by 30%. The results for the cases of single damage are shown in Figure 5(a–c). Detection of multiple damage is shown in Figure 5(d–f). From Figure 5, it can be observed that there is a small deterioration in the accuracy of the damage size prediction due to the non-linear relationship between frequency changes and damage. Furthermore, in all cases but case 12 the magnitude of damage was underpredicted because the sensitivity coefficients were derived around the original structure, which also indicates that the large changes in the

flexibility cannot be predicted as closely as small ones. Despite this, the true damage locations were still predicted reasonably well.

4.2. EXAMPLE 2: A PERIODIC MASS–SPRING STRUCTURE OF 20 ELEMENTS

In this example, the mass and stiffness of each element of the 20-element mass spring system are $2{\cdot}0 \times 10^5$ kg and $3{\cdot}3636 \times 10^8$ N/m respectively. The cases of changes, 5 and 30%, in the flexibility of elements 1, 10 and 20 are also considered as the light and severe damages respectively.

It is well recognized that the search for the optimum solution from equation (33) can be computationally expensive if the structure is complex and the number of potential damaged sites is large, and an erroneous solution may even appear if the number of available measured frequencies is not sufficient. In other words, a significant time saving and improvement in the accuracy of the solution can be achieved if it is possible to limit the search to a subset of possible damage sites.

The results from sensitivity analysis shown in Figure 3 indicate that the change of a specified natural frequency is more sensitive to damage at some locations than at others; in other words, damage at a particular location induces larger changes in some natural frequencies than in others. That is, if the large differences only in the natural frequencies are used, the damaged locations which have the greatest influence can be detected. Following this principle, the preliminary detection in Example 1 successfully identified a few of possible damaged locations. It might be expected that this approach could identify the damage site correctly for a single-damage case. In multiple-damage situations, there is a risk of losing one or more damaged sites if insufficient modes are used and their frequencies change appreciably. However, if sufficient modes are considered, the list of possible damage sites can be large enough to minimize this risk.

Since the computational time and core memory size depend on the number of periodic elements, the alternative way for improving the computational efficiency is to make full use of the substructure concept. In this substructure-based method, each substructure which is composed of several mass–spring elements forms the basic periodic element, thus, the number of periodic element is reduced. For example, for the 20-element periodic mass–spring system, if each substructure consists of two mass–spring elements, the number of periodic elements (i.e., the number of substructures) becomes 10; if each substructure includes four mass–spring elements, the number of periodic elements becomes five. Reduction of the number of periodic elements improves the computational efficiency; furthermore, the degree of accuracy of damage location detection can be improved because the amount of available modal test data becomes nearer to the reduced number of periodic elements.

To illustrate the benefits of the two ways developed herein, 12 cases of 5 and 30% flexibility increases in one or multiple elements are considered (shown in Table 3). Once again, the changes in the first five natural frequencies are used as the only known variables towards the detection of the location and magnitude of the damage. The calculated changes in the five natural frequencies produced by the 12 damaged scenarios are shown in Table 4.

From the % frequency differences listed in Table 4, all the potential damage locations can be determined by using the sensitivity variation shown in Figure 3(b). From Table 2, in cases 1, 4, 5, 6, 7, 10, 11 and 12, all the differences in the five frequencies are large; thus, the six elements with the highest sensitivities for either of the five natural frequencies should be considered as the potential damage locations. On the other hand, for cases 3 and 9, all the differences in the five frequencies are small; that is, the possible damage locations are the six

TABLE 3

Damage scenarios for the 20-element periodic mass–spring structure

Cases	Case 1	Case 2	Case 3	Case 4	Case 5	Case 6	Case 7	Case 8	Case 9	Case 10	Case 11	Case 12
Damage element												
	1	10	20	1, 10	1, 20	1, 10, 20	1	10	20	1, 10	1, 20	1, 10, 20
$\delta\xi$	5%						30%					

TABLE 4

The changes in the first five natural frequencies due to damage for the 20-element periodic mass–spring structure

Mode	Relative change of the natural frequencies in percentage due to damage											
	Case 1	Case 2	Case 3	Case 4	Case 5	Case 6	Case 7	Case 8	Case 9	Case 10	Case 11	Case 12
1	− 0·24	− 0·14	0·00	− 0·25	− 0·38	− 0·38	− 1·44	− 0·81	− 0·01	− 2·21	− 1·45	− 2·22
2	− 0·24	− 0·08	− 0·01	− 0·25	− 0·32	− 0·33	− 1·41	− 0·48	− 0·08	− 1·91	− 1·48	− 2·00
3	− 0·23	− 0·19	− 0·03	− 0·27	− 0·42	− 0·45	− 1·36	− 1·11	− 0·21	− 2·37	− 1·56	− 2·57
4	− 0·22	− 0·03	− 0·06	− 0·29	− 0·26	− 0·32	− 1·28	− 0·20	− 0·41	− 1·57	− 1·67	− 1·93
5	− 0·21	− 0·23	− 0·10	− 0·31	− 0·44	− 0·54	− 1·19	− 1·33	− 0·65	− 2·42	− 1·81	− 3·04

elements with the lowest sensitivities for either of the five frequencies. In cases 2 and 8, only the differences in the first, the third and fifth frequencies are large; similarly, the six elements where the disorder produces largest difference in the corresponding natural frequencies are referred to as the potential damage locations. Examining all the modes showing the largest frequency changes, and identifying six locations with the highest damage sensitivities for each, gave a list (after eliminating duplicates) of possible damage sites shown in the column of method 1 of Table 5.

Now consider a substructured model of the 20-element system when divided into periodic systems each containing four of the actual masses and their springs. Each substructure will be represented by a single equivalent mass equal to four of the actual masses, together with a single spring. The equivalent stiffness of the spring is chosen such that the fundamental frequency of the mass–spring model is equal to the fundamental frequency of the actual-mass–spring substructure. Thus, the computed change of flexibility becomes the corresponding change of equivalent flexibility of the substructure, which also indicates the degree of damage of the substructure and the potential damage locations of the original periodic system. For example, the change of equivalent flexibility of the second substructure indicates that elements 5, 6, 7 and 8 of the original system are the potential damage locations. Similarly, if one substructure only includes two mass–spring elements, the 20-element periodic structure becomes a periodic system with 10 substructures. The calculated change of the equivalent flexibility of the substructure provides a greater number of possible sites at which the damage may exist. That is, for example, the change of equivalent flexibility of the second substructure indicates that element 3 or 4, or both of them of the original system are possibly damaged. After the potential damage locations are identified, the magnitude of the damage can be obtained by solving the optimum equation (33).

TABLE 5

The potential damage locations of the 20-element periodic mass–spring structure identified by different methods

Case	Method 1: sensitivity analysis	Method 2: one substructure consisting of two elements	Method3: one substructure consisting of four elements
1, 7	All the elements except elements 11 and 20	1, 2	1, 2, 3, 4
2, 8	All the elements except elements 7, 11, 13, 15 and 20	1, 2, 9, 10	1, 2, 3, 4, 9, 10, 11, 12
3, 9	11, 20	19, 20	5, 6, 7, 8, 17, 18, 19, 20
4, 10	All the elements except elements 11 and 20	1, 2, 9, 10	1, 2, 3, 4, 9, 10, 11, 12
5, 11	All the elements except elements 11 and 20	1, 2, 19, 20	1, 2, 3, 4, 17, 18, 19, 20
6, 12	All the elements except elements 11 and 20	1, 2, 9, 10, 19, 20	1, 2, 3, 4, 9, 10, 11, 12, 17, 18, 19, 20

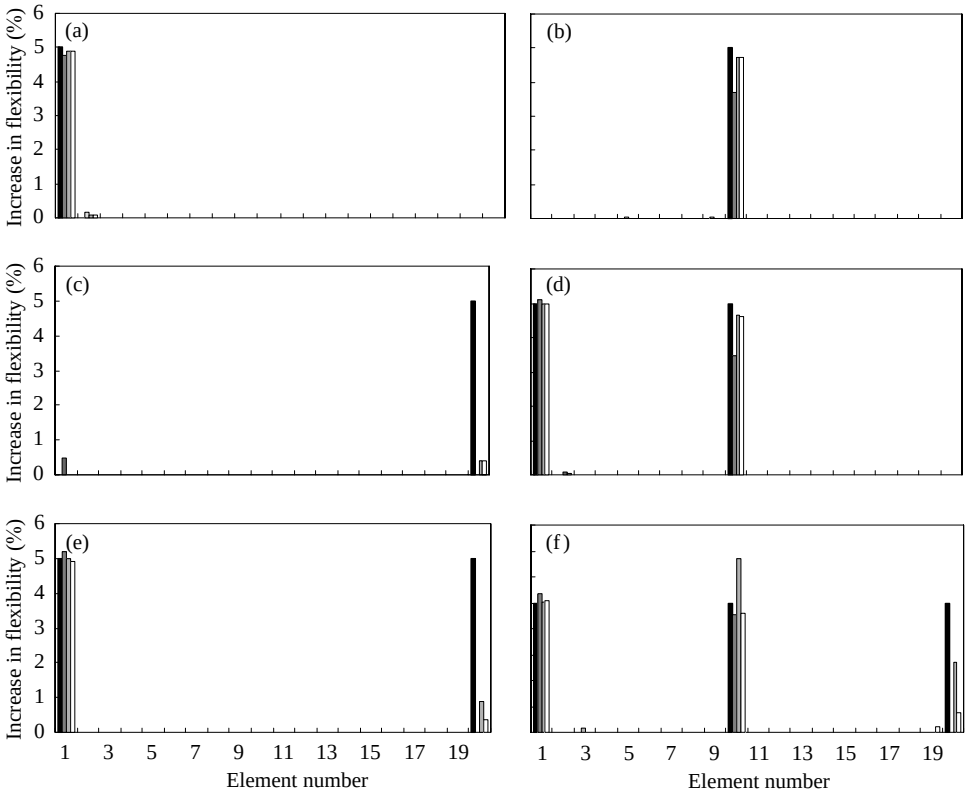

Figure 6. Detection of light damage of the 20-element periodic mass–spring structure at: (a) element 1, (b) element 10, (c) element 20, (d) elements 1 and 10, (e) elements 1 and 20, (f) elements 1, 10 and 20: ■, actual damage; ■, method 1; □, method 2; □, method 3.

Table 5 shows the potential damage locations identified by different methods. From the table, it can be seen that only a few elements for each case were excluded by method 1 as the number of examined modes and locations is large enough to avoid the loss of possible

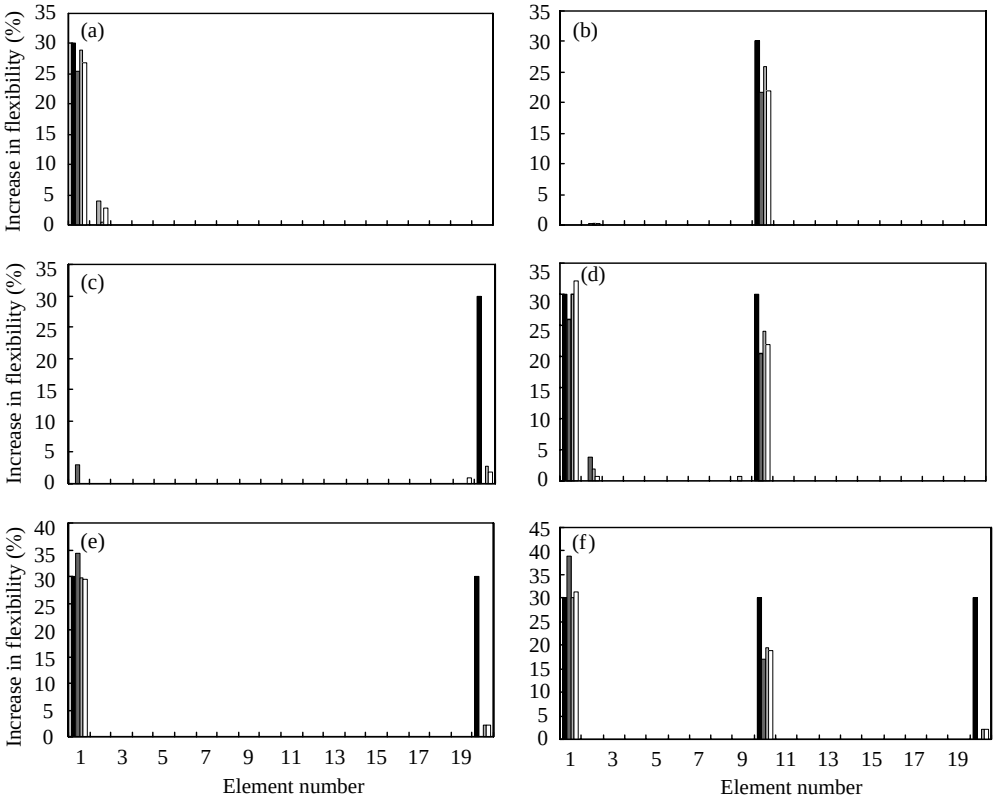

Figure 7. Detection of severe damage of the 20-element periodic mass–spring structure at: (a) element 1, (b) element 10, (c) element 20, (d) elements 1 and 10, (e) elements 1 and 20, (f) elements 1, 10 and 20: ■, actual damage; ▩, method 1; ▨, method 2; □, method 3.

damage locations. Specifically, in each case element 20 is excluded by method 1 since it has little effect on the first five frequencies. Methods 2 and 3 making full use of the advantage of substructure gave location lists which were distinguishable from method 1. In method 2, the search lists were reduced to not more than six locations, in some cases only to 2 locations. In method 3, except cases 6 and 12, the number of identified possible damage locations did not exceed 8. Since the number of locations used for each search of solution is reduced, the computational time required is also saved.

The magnitudes of the damage calculated from equation (33) corresponding to a 5% increase in the flexibility of single and multiple elements are shown in Figure 6. Figure 6(a) shows that some of the damage of element 1 is allocated to element 2 since element 2 has the same sensitivity to some frequencies as element 1. Figure 6(e, f) shows that the identification of the damage of element 20 is relatively difficult as element 20 has low degree of sensitivity to the first five natural frequencies. In general, the identification of light damage occurring at any location except at the free end of the system is very successful. Moreover, method 2 not only gives a more accurate prediction of both the damage sites and magnitude, but also improves the computational efficiency more effectively.

Detection of a 30% increase in flexibility in elements 1, 10 and 20 is shown in Figure 7(a–c) respectively. The location of damage was calculated correctly for elements 1 and 10, and the magnitude of damage for element 10 is slightly underpredicted. Once again, both the damage location and the magnitude for element 20 cannot be identified correctly. Multiple severe damage with a 30% increase in flexibility occurring in elements 1,

10 and 20 is shown in Figure 7(d–f). The location and the magnitude of the damage for element 1 were predicted accurately, the location of damage for element 10 was predicted successfully while the magnitude of damage for element 10 was underpredicted by more than 20%. As expected, the damage of element 20 could not be predicted correctly.

5. CONCLUSIONS

The sensitivities of natural frequencies to the location of disorder in flexibility of mono-coupled periodic structures were obtained by using the characteristic receptance method and presented as a set of undetermined equations. The optimum solutions of these equations provided reliable information about the locations and size of damage at one or more sites. The proposed approach simplifies the computation of the structural sensitivities by making full use of the repetitive elements in periodic systems, and also has the practical attraction of only requiring information about the changes in a few of the natural frequencies between the undamaged and damaged states. Furthermore, if the periodic structure is simplified as a periodic mass–spring system, the sensitivity matrix can be determined by the total number of periodic elements, and it does not depend on structural parameters such as stiffness and mass. That is, the identification of the location of damage based on the sensitivity analysis depends only on the total number of periodic elements and the difference in the natural frequencies between the undamaged and damaged states, thus it does not require any prior information such as the stiffness and mass on the undamaged structures. Since the natural frequencies in the undamaged or damaged state can be measured, and the number of periodic elements is easily available, the proposed method becomes feasible in practice.

This proposed method was applied to the identification of damage in 10- and 20-element periodic mass–spring structures. In the application, the changes in the first five natural frequencies were used as the only known variables. In general, the method provided good predictions of both the location and the content of damage at one or more sites. Light damage, in the order of 5% increase in the flexibility, was identified accurately. The location of severe damage, 30% increase in the flexibility, was also identified extremely accurately, but the magnitude of such severe damage in some cases was underpredicted. However, damage of the elements that have low sensitivity to the first five natural frequencies, such as the 20th element in the 20-element periodic structure, could not be identified correctly. Since only five natural frequencies are needed, the requirement for practical measurement is modest.

The substructure method has been proposed to improve the computation efficiency, which limits the search of optimum solutions to a subset of potential damage sites, thus a significant time saving can be obtained. Besides that, numerical analysis from the two examples mentioned above shows that the substructure method generally gives better results.

It must be emphasized that the type of system considered here is rather simple when compared to most real periodic engineering structures. However, the present study allows a number of physical insights to be made from a structural damage detection point of view. Nonetheless, there are still some matters to be investigated before this proposed approach becomes a truly variable method of damage detection in periodic structures; how the approach performs in practice when the actual measurements contain noise; how the approach may be modified to accommodate both the incomplete measured natural frequencies and mode shapes; how the approach performs for periodic systems with complex boundary conditions; how the approach performs for multi-coupled periodic systems or near periodic systems.

ACKNOWLEDGMENTS

This research was funded jointly by the National Natural Science Foundation of China (Grant No. 59908003) and the Natural Science Foundation of Hubei province (Grant No. 99J035). The supports are greatly appreciated and helpful suggestions from the reviewers are also acknowledged.

REFERENCES

1. D. J. MEAD 1996 *Journal of Sound and Vibration* **190**, 495–524. Wave propagation in continuous periodic structures: research contributions from Southampton, 1964–1995.
2. P. W. ANDERSON 1958 *Physical Review*: *A Journal of Experimental and Theoretical Physics* **109**, 1492–1505. Absence of diffusion in certain random lattices.
3. D. J. MEAD and A. S. BANSAL 1978 *Journal of Sound and Vibration* **61**, 481–496. Mono-coupled periodic systems with a single disorder: free wave propagation.
4. G. J. KISSEL 1988 *Ph.D. Dissertation*, *Massachusetts Institute of Technology*. Localization in disordered periodic structures.
5. K. ISHII 1973 *Supplement of the Progress of Theoretical Physics* **45**, 56–86. Localization of eigenstates and transport phenomena in the one-dimensional disordered system.
6. D. C. HERBERT and R. JONES 1971 *Journal of Physics C*: *Solid State Physics* **4**, 1145–1161. Localized states in disordered systems.
7. D. J. THOULESS 1972 *Journal of Physics C*: *Solid State Physics* **5**, 77–81. A relation between the density of states and range of localization for one dimensional random systems.
8. G. Q. CAI and Y. K. LIN 1991 *American Institute of Aeronautics and Astronautics Journal* **29,** 450–456. Localization of wave propagation in disordered periodic structures.
9. S. D. LUST, P. P. FRIEDMANN and O. O. BENDIKSEN 1990 *Proceedings of the* 31st *AIAA Dynamics Conference*, *Long Beach*, *CA*, *AIAA Paper* 90-1214. Mode localization in multi-span beams.
10. J. V. ARAUJO DOS SANTOS, C. M. MOTA SOARES, C. A. MOTA SOARES and H. L. G. PINA 2000 *Computers and Structures* **78**, 283–291. A damage identification numerical model based on the sensitivity of orthogonality conditions and least squares techniques.
11. H. P. CHEN and N. BICNIC 2000 *Computers and Structures* **74**, 559-570. Assessment of damage in continuum structures based on incomplete modal information.
12. S. F. MASRI, A. W. SMYTH, A. G. CHASSIAKOS, T. K. CAUGHEY and N. F. HUNTER 2000 *American Society of Civil Engineers Journal of Engineering Mechanics* **126**, 666-676. Application of neural networks for detection of changes in nonlinear systems.
13. C. R. FARRAR and K. M. CONE 1995 *Proceedings of the* 13*th International Modal Analysis Conference* Vol. 1, 203–209. Vibration testing of the I-40 bridge before and after the introduction of damage.
14. S. HASSIOTIS and G. D. JEONG 1993 *Computers and Structures* **49**, 679-691. Assessment of structural damage from natural frequency measurements.
15. D. CAPECCHI and F. VESTRONI 1999 *Earthquake Engineering and Structural Dynamics* **28**, 447–461. Monitoring of structural systems by using frequency data.
16. M. BISWAS, A. K. PANDEY and M. M. SAMMAN 1990 *The International Journal of Analytical and Experimental Modal Analysis* **5**, 33–42. Diagnostic experimental spectral/modal analysis of a highway bridge.
17. P. CAWLEY and R. D. ADAMS 1979 *Journal of Strain Analysis* **14**, 49–57. The location of defects in structures from measurements of natural frequencies.
18. N. STUBBS, T. H. BROOME and R. OSEGUEDA 1990 *American Institute of Aeronautics and Astronautics Journal* **28**, 146–152. Non-destructive construction error detection in large space structures.
19. J. E. LUCO, H. L. WONG and A. MITA 1992 *Earthquake Engineering and Structural Dynamics* **21**, 525–541. Active control of the seismic response of structures by combined use of base isolation and absorbing boundaries.
20. G. H. GOLUB and C. VAN LOAN 1983 *Matrix Computations*. Baltimore: Johns Hopkins University Press.